Topological controls on catchment-scale sediment dynamics

Yasmin Walley*[1], Alexander J. Henshaw[1]
[1] School of Geography, Queen Mary University of London, London, United Kingdom
* Corresponding Author – y.r.s.walley@qmul.ac.uk

Article accepted for publication in Earth Surface Processes and Landforms on 31st October 2022

Abstract

The episodic transfer of sediment from source to sink is a fundamental process in fluvial systems that influences river morphology, aquatic and riparian ecosystems, and risk from a variety of associated natural hazards. The hierarchical structure of river networks has been identified as a key control on spatiotemporal patterns of sediment routing at the catchment-scale, but very few studies have systematically explored this relationship. In this paper, we investigate the role that drainage network topology plays in modulating sediment flux and morphodynamic activity. We simulate the geomorphological responses of four topologically distinct catchments from New Zealand's South Island to sequences of flood events using a landscape evolution model. Spatiotemporal variation in different types of geomorphological activity is assessed via a link-based framework, and potential interrelationships between within-network changes and discharge and sediment yield at the catchment outlets are explored to provide insights into relative levels of network connectivity. We also investigate the occurrence of geomorphic 'hotspots' in relation to network topology, and their impact on the downstream transfer of sediment in different network 'types'. Dissected networks were found to exhibit much greater spatiotemporal variability in geomorphological activity compared to narrow, elongated networks where change was concentrated in mainstem reaches. The frequency and significance of geomorphological hotspots are shown to vary between network types, with strong contrasts evident between dissected networks with steep topography and elongated networks with more gentle gradients. Dissected networks exhibited mostly non-linear relationships between within-network geomorphological activity and outlet discharge and sediment yield. However, moderate-strong linear relationships between these variables were observed in mainstem-dominated networks, indicating much greater levels of connectivity across a range of flow conditions. We discuss the implications of these findings on the transformation of environmental signals through fluvial systems with different topological structures, and the differential responses of catchments to disturbance events.

Keywords: *Sediment Dynamics, Network Topology, River Networks, Catchment Modelling, CAESAR-Lisflood.*

1.0 INTRODUCTION

The episodic transfer of sediment from source to sink is a fundamental process in fluvial systems. Driven by water flow and controlled by the regional characteristics of climate, geology, tectonics and landscape history, the sediment regime significantly influences river morphology, water quality, responses to system disturbance, and the distribution of habitats (Schumm, 1977; Brierley and Fryirs, 2005; Burt and Alison, 2010). Sediment transport is consequently well researched across a variety of spatial and temporal scales, but the complexity of fluvial systems and a lack of efficient analytical tools have impeded a comprehensive understanding of catchment-scale sediment flux. This complexity is largely driven by the highly nonlinear relationship that exists between sediment flux and water flow (Coulthard and Van De Wiel, 2007), in which the same volume of water flowing through a given reach can alternately generate erosion, deposition, or no response at all. This lack of understanding is exacerbated at the catchment scale, which has traditionally been neglected in favour of reach and local scales which are more straightforward to study.

Research into the downstream transfer of sediment has historically focused on the localised transport of grains and the movement of individual sediment pulses through a reach (e.g. Lisle et al., 2001; Sklar et al., 2009; James, 2010), particularly the relative significance of dispersion and translation processes (e.g. Meade, 1985; Knighton, 1989; Lisle et al., 2001). Other studies have explored the impact of intersecting tributaries or 'tributary-trunk' dynamics (e.g. Knighton, 1980; Rice, 1998), focusing on the impact of tributaries on the downstream trunk channel with regards to grain size characteristics and downstream fining (e.g. Church and Kellerhals, 1978; Knighton, 1980; Dawson, 1988; Rice and Church, 1998). Relatively few studies have attempted to develop these concepts at the catchment scale, with some exceptions exploring the catchment-scale distribution of significant confluences (Benda et al., 2004a; Benda, 2008; Rice, 2017), and the influence of network structure in modulating sediment waves (Benda et al., 2004b; Sklar et al., 2006, 2009; Gran and Czuba, 2017). More recently, studies have explored the role of geomorphic 'hotspots' as key nodes in the river network predisposed to changes in storage and geomorphic change (Czuba and Foufoula-Georgiou, 2014, 2015; Walley et al., 2018). Network topology emerges from this literature as a key element in organising catchment-scale sediment flux, but only the work of Walley et al. (2018) systematically compares how different network structures impact patterns of sediment routing, highlighting the role of regional characteristics in governing both network configuration and sediment flux.

Analysing catchment-scale sediment transfer thus necessitates consideration of the underlying network topology, and the associated regional-scale processes. Over much longer timescales, the same processes which control regional sediment transfer also determine the topology of river networks at the catchment scale, such as the tectonic and climatic settings that establish topology during initial mountain building, and continue to evolve networks over time (Hovius et al., 1998; Castelltort et al., 2012; Viaplana-Muzas et al., 2015). This relationship between topology and regional processes is thus key to understanding catchment-scale sediment flux; however, the complex relationships and the spatial and temporal scales over which these processes occur make them difficult to understand or quantify. Previous approaches to catchment-scale analysis have employed the network structure as a tool to organise system complexity, most notably in the form of stream ordering frameworks (e.g. Horton, 1945; Strahler, 1957; Shreve, 1967) and their associated derivatives (e.g. Tokunaga, 1978; Benda et al., 2004b; Zanardo et al., 2013; Heasley et al., 2019). Walley et al. (2020) employ these metrics to classify 59 catchments in the South Island of New Zealand into five 'types', identifying a clear relationship between network topology and regional setting.

The resulting network classifications are used in this study to investigate the role that drainage network topology plays in modulating the spatio-temporal pattern of sediment transfer from source to sink. While quantitative frameworks exist which utilise DEM and remote sensing-derived indices to characterise catchment-scale sediment connectivity and landform evolution (e.g. Bracken et al., 2015; Brierley et al., 2006; Heckmann et al., 2018), a numerical modelling approach was deployed here to enable a greater degree of experimental control and exploration of effects over large spatio-temporal scales. The CAESAR-Lisflood model was identified as a fit-for-purpose catchment-scale application, which simulates sediment transfer and morphodynamic adjustment in a computationally efficient manner, with a good degree of process replication. The model is also capable of large-scale simulations over 100s-1000s of years and 100s of km^2 (Coulthard et al., 2013), and given the difficulty of validating catchment-scale models with real-world data, CAESAR-Lisflood was additionally chosen as a well-known landscape evolution model (LEM) that is established in the literature (Coulthard et al., 2013; Hancock et al., 2015, 2017; Coulthard and Skinner, 2016; Liu and Coulthard, 2017; Xie et al., 2018). We thus use CAESAR-Lisflood in this paper to examine the distribution and modulation of sediment movement through topologically distinct networks and establish whether there are key differences in the emergent sediment pathways. Potential inter-relationships between geomorphological activity within the different networks and discharge and sediment yield at their outlets are explored to provide further insight to network connectivity. We also investigate the occurrence of geomorphic 'hotspots' in relation to network topology, and their impact on the downstream transfer of sediment in different network 'types'.

2. TOPOLOGICALLY DISTINCT NETWORK STRUCTURES

The network classifications identified by Walley et al. (2020) were used to select topologically representative catchments in which modelled spatio-temporal patterns of sediment connectivity could be compared. The five network 'types' are distinguished by catchment topography and network structure (Fig. 1), in which types A, B, D and E exhibit values along the extremities of each axis. These groupings are characterised by distinct topological properties (Table 1), while the catchments in Type C reflect a mixture of topologies with elements from the other types. It was assumed that the greatest contrast in sediment routing patterns would occur between the outermost network 'types', and Type C was consequently removed from further analysis. The representative networks from the remaining 'types' identified by Walley et al. (2020) were evaluated for this study, but the data necessary to parameterise the CAESAR-Lisflood model was only available in the Type A catchment. The networks from the Type B, D and E clusters were thus replaced with those that fell closest to the centre of the cluster for which the necessary data was obtainable.

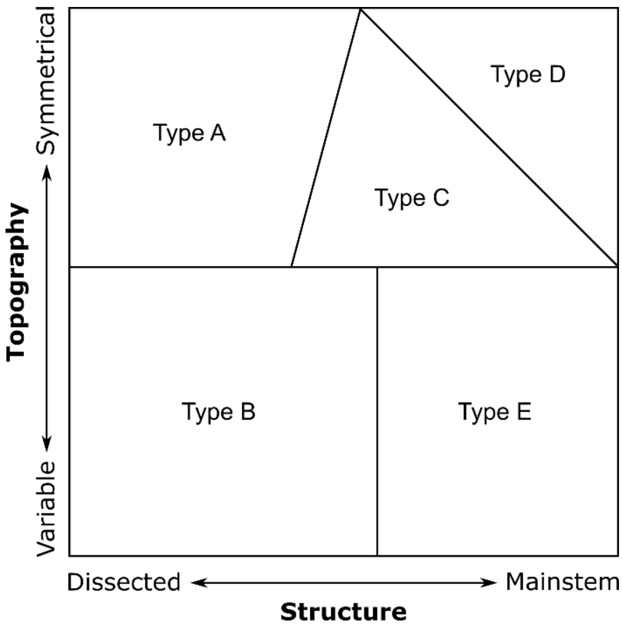

Figure 1. Simplified representation of AHC clusters, and summary characteristics of the principal components. From Walley et al. (2020).

Table 1. Parameter values summarised in each class identified by the AHC analysis. From Walley et al. (2020).

Class	Strahler Order (Ω) *Median*	Network Branching (c)	Width Ratio	Elevation Ratio	Drainage Density (km/km^2)	Confluence Angle (°) *Mean*
A	6	Low	Wide Headwaters	Moderately Gentle	Mid	72.6
B	5	Low	Wide Headwaters and Consistent Width	Moderately Steep	High	64.5
C	5	Mid	Wide Headwaters and Consistent Width	Moderate	Mid	72.0
D	4	High	Consistent Width	Moderately Gentle	Low	78.3
E	4	High	Consistent Width	Steep	High	66.1

The four identified study catchments were evaluated in the same manner as Walley et al. (2020), to establish the internal characteristics of the catchment topography and network structure. The Type A network was identified by Walley et al. (2020) as the Motueka River, which exhibits a dissected network structure, with wide headwaters narrowing towards the outlet (Fig. 2a & e). The catchment is relatively large and contains symmetrical gentle-moderate slopes (Fig. 3a & e) which steepen towards the western boundary. This network is similar in structure to the South Ashburton River which represents the Type B catchments, and also contains a branching, dissected network topology (Fig. 2a & b). The South Ashburton catchment is smaller than the Motueka and does not extend upstream into the Southern Alps, so the topography exhibits gentle slopes and very wide valley floors (Figs. 2j, 3f). Both catchments are relatively rounded in shape and neither exhibit a prominent mainstem, suggesting that patterns of sediment routing are likely to be dominated by geomorphic hotspots at key confluences (Benda et al., 2004b; Rice, 2017; Walley et al., 2018).

The Waiau Toa/Clarence River represents the Type D catchments and is the largest of the four study networks. In contrast to the Motueka and South Ashburton catchments, the Waiau Toa/Clarence River has an elongate shape and relatively consistent width (Fig. 2c & g), resulting in a prominent mainstem and increasing network symmetry in the headwaters (Fig. 3g).

The Waiau Toa/Clarence network is additionally characterised by drainage anomalies, including river bends of more than 90°, tributaries joining the network oriented in an upstream direction, and parts of the river which flow laterally across mountain ranges (Duvall et al., 2020). These anomalies reflect the highly active tectonic landscape and indicate a history of river capture across the region. The Waihao River, which represents the Type E catchments, contains two elongate subcatchments which exhibit the same narrow, mainstem-dominated structure as the Waiau Toa/Clarence network (Fig. 2d). It does not exhibit the same tectonic influence, however, and has a gentler topography similar to the South Ashburton catchment. The patterns of sediment routing are likely to be strongly influenced by the mainstem channels in these catchments, and exhibit geomorphic hotspots at the head of the mainstem reaches (Benda et al., 2004b; Rice, 2017; Walley et al., 2018).

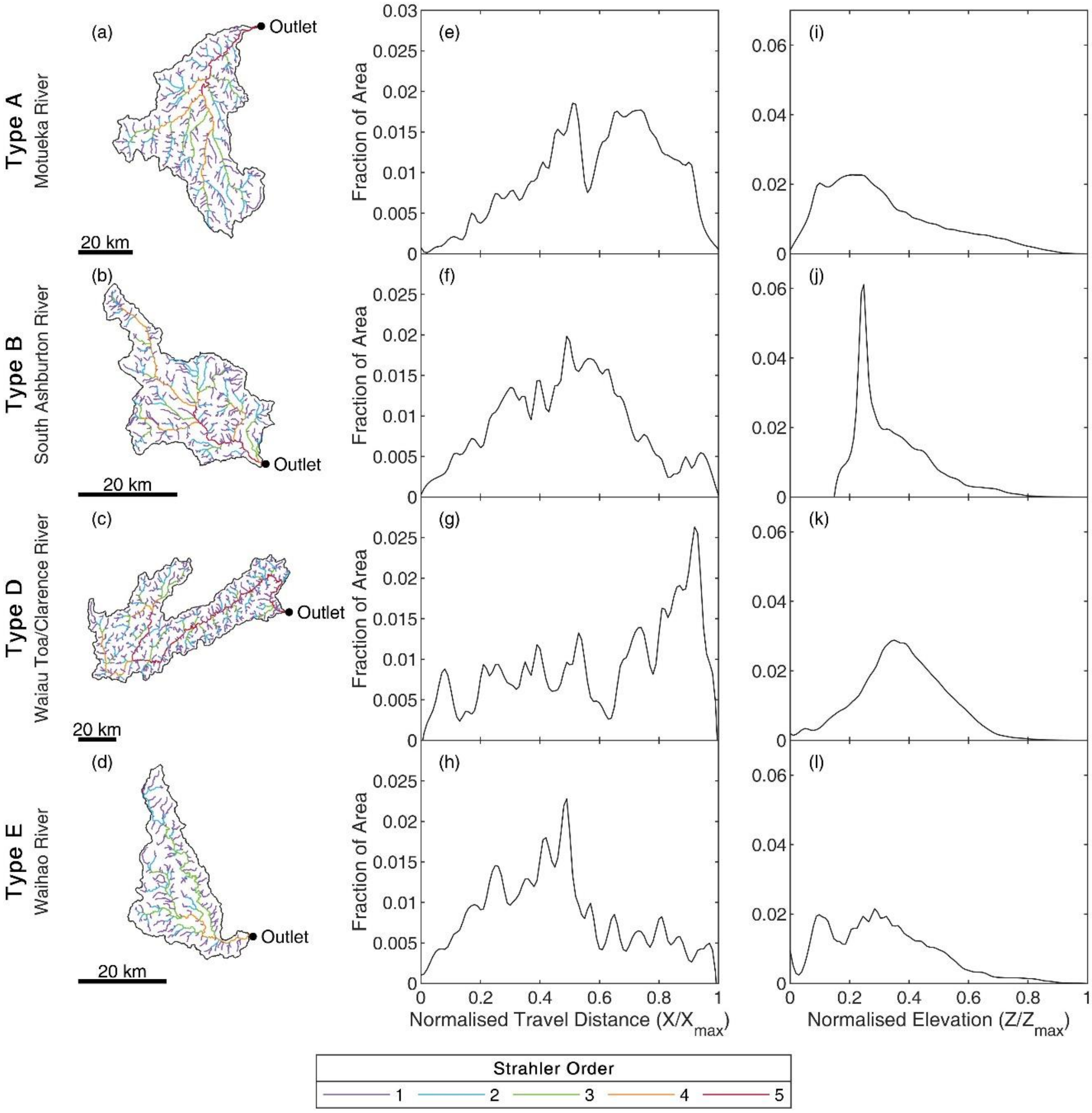

Figure 2. Internal catchment structure of the four study catchments. (a-d) Network map indicating Strahler orders, (e-h) Width function, a normalised frequency distribution of travel distance to the outlet, and (i-l) Hypsometry function, a normalised frequency distribution of elevation. Binning increments for the width and hypsometry functions were 1/50 of maximum value.

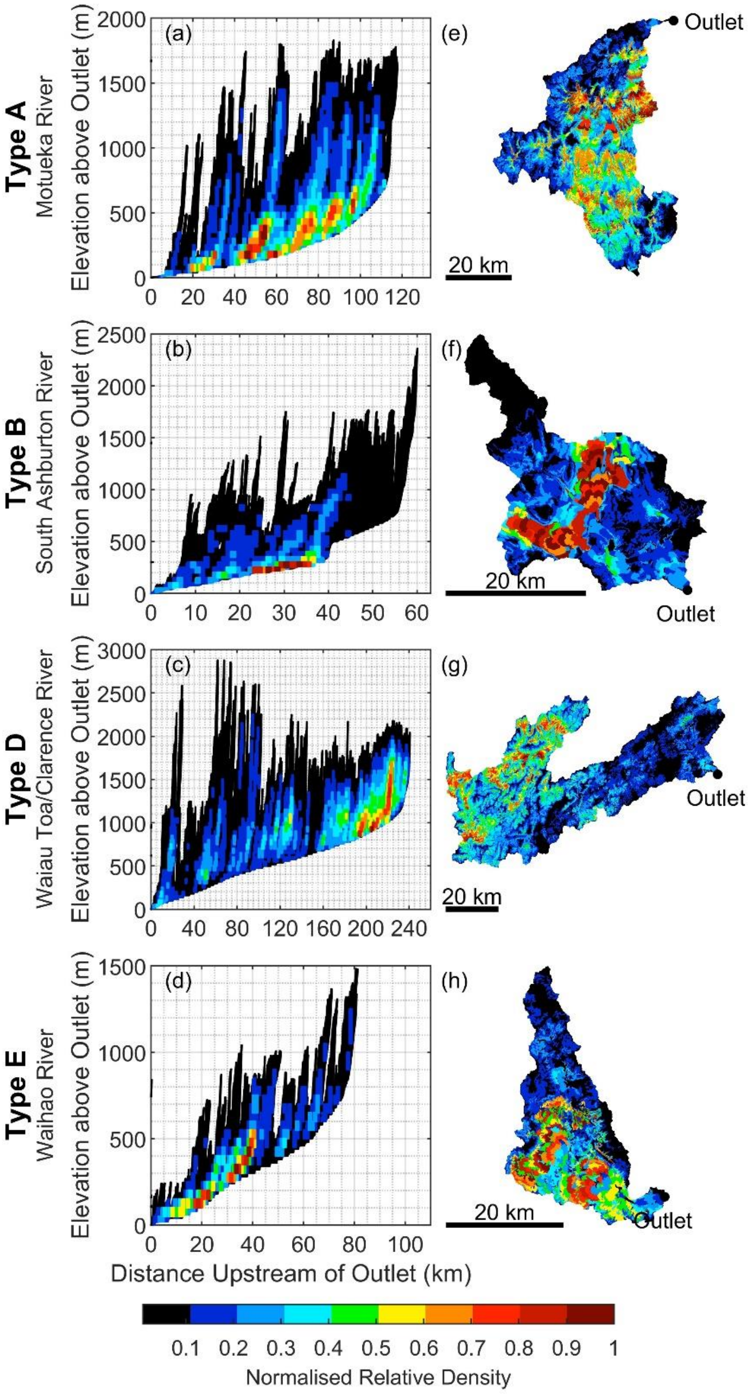

Figure 3. Distribution of elevation and travel distance for (a-d) every point in the catchment binned in a bivariate frequency distribution, showing the relative density of cells. (e-h) display the data from a-d as a catchment map. The values of highest density occur where multiple points in the network exhibit the same values of both elevation and distance upstream of the outlet. The colours are normalised on each set of figures.

3. THE CAESAR-LISFLOOD MODEL

To explore patterns of sediment flux at the catchment scale, the four identified topologically dissimilar networks were simulated using the CAESAR-Lisflood LEM (Coulthard et al., 2000, 2002, 2005, 2013). CAESAR-Lisflood simulates landscape evolution by moving water over a DEM, and uses fluvial and slope processes to calculate erosion and deposition in each cell for each timestep (Coulthard et al., 2013). In catchment-scale simulations a 'real-time' rainfall input is used to calculate runoff, which is routed using the LISFLOOD-FP 2D inertial flow model and used to calculate flow depth and velocity in each grid cell. These are in turn used to calculate fluvial erosion and deposition in up to nine grainsize fractions, with a method of storing sub-surface sediment in layers allowing for vertical grainsize variability. Slope processes additionally allow for the erosion of sediment into the fluvial system via soil creep and mass movements, the latter triggered when a critical slope threshold is exceeded. A catchment-scale simulation in CAESAR-Lisflood thus requires a DEM of the study catchment and a timeseries of hourly rainfall rates as the two primary inputs, which must be set up to maximise output detail, while also allowing for realistic model run times. The resolution of the DEM determines the number of calculations required for each timestep and must be considered alongside the length of the rainfall input, as shorter simulations can be carried out at higher resolutions. It is also necessary to identify the *m* value which controls the peak and duration of simulated hydrographs (Beven and Kirkby, 1979; Beven, 1997), which can be calibrated against hydrological gauge data.

3.1 Parameterisation and Validation

The surface DEM is one of the key components of the CAESAR-Lisflood model, and the balance between catchment size and grid resolution is a key consideration for parameterisation. Rescaling each DEM to an appropriate cell size has significant implications for the simulations, as a linear increase in resolution results in an exponential increase in the number of grid cells and a greater than exponential increase in simulation time. High resolutions can also cause steeper slopes between cells and thus greater potential for erosion and deposition. Finding an appropriate resolution depends on the size of the study catchment, as CAESAR-Lisflood is best suited to applications with resolutions below 100 m and less than 500,000 cells. Surface data for the study catchments was therefore taken from a mosaicked 8m DEM (Geographx, 2012), and resampled to the smallest resolution which produced a DEM containing less than 250,000 cells, or 500,000 cells where the smaller value was not possible (Table 2). An appropriate slope failure threshold was identified by running sensitivity tests in CAESAR-Lisflood for one simulation day, to identify the lowest value which would not produce widespread hillslope failure within the first few iterations. Bedrock DEMs were produced by subtracting 1 m from the entire surface, which act to prevent excessive and unrealistic incision occurring in steeper channel sections during simulations (Hancock et al., 2011). In the absence of spatial data on bedrock depth, an erodible layer of constant thickness was specified to ensure a significant reservoir of material was available for erosion and transport through the networks.

Table 2. Resolution and number of grid cells for each catchment DEM.

Catchments	Cell Size (m)	Number of Cells
Motueka River	96	457,452
South Ashburton River	72	230,720
Waiau Toa/Clarence River	120	481,600
Waihao River	72	234,624

The simulated grain size distribution is also a key consideration during parameterisation, as different fractions are transported over different scales through the network. Complex relationships exist between grain size and the rate of entrainment and transport, deposition and layering within sediment stores, and bed armouring on the surface, which have significant implications for the spatio-temporal scales of sediment connectivity. Although CAESAR-Lisflood has the capacity to model multiple grain size fractions simultaneously, it cannot trace the spatio-temporal pathways of these fractions through the network in a single simulation, which would require individual simulations for each fraction with the assumption that transport is unaffected by grain size interaction. In addition, catchment-specific grain size distributions were not available in the necessary spatial or temporal resolutions in any of the study catchments. The model was therefore run using a single representative grain size fraction in order to isolate the catchment-scale sediment pathways in each catchment, and directly compare these patterns between their topologically distinct structures. Given the relatively steep, active nature of rivers in the South Island of New Zealand, sediment smaller than 2 mm was assumed to be fully transported in suspension and was subsequently excluded from this analysis. Gravel bedload was assumed to be the dominant grain size in active transport. Representative values were taken from the midpoint of common diameter ranges for fine, medium, and coarse gravel, and test simulations identified the fine gravel value of 5 mm to transport sufficient volumes within realistic simulation times.

The final element of parameterising the CAESAR-Lisflood model is the hourly rainfall input, which is converted into discharge and routed through the channel network. One of the primary parameters in the hydrological model is therefore the *m* value, the parameter which controls the magnitude and duration of the hydrograph for each rainfall event (Beven, 1997). This value can be calibrated from the master recession curve (MRC) of a hydrological gauge dataset from the catchment of interest (Lamb and

Beven, 1997). Discharge timeseries were thus obtained from automatic gauging stations in each study catchment, and rainfall timeseries acquired from the closest rainfall gauge. A continuous timeseries of discharge and rainfall was then generated by matching the dates from these datasets, and the *m* value calculated using the method of Lamb and Beven (1997). Appropriate recession curves were first manually identified from the discharge record as those with minimal recharge from rainfall events, and of at least 4 days duration (Fig. 4a). Each curve was then shifted along an arbitrary timeline relative to the other recession curves until a good alignment was found (Fig. 4b), and the parameters of the MRC were calculated by visually calibrating the smoothed line of best fit (Fig. 4c). A value for *m* was then estimated from the gradient of the relationship between discharge per unit area and relative storage deficit (Table 3), in which the latter was calculated by cumulatively summing discharge per unit time with the deficit at peak discharge assumed to be zero (Lamb and Beven, 1997).

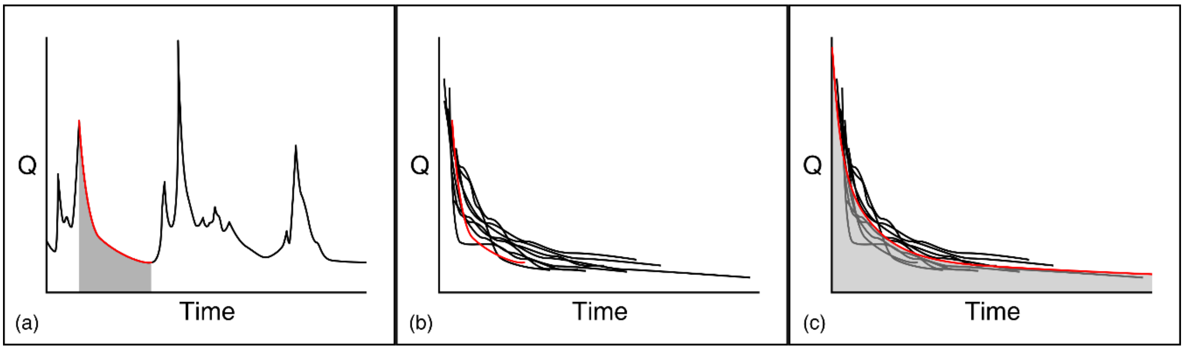

Figure 4. Method of calculating the Master Recession Curve (MRC). (a) Recession curves are manually selected from the discharge record, then (b) the recession curves are aligned along an arbitrary timeline, and (c) the MRC parameters are calculated from a line of best fit.

Table 3. m *values for each catchment.*

Catchments	***m* Value**
Type A	0.028
Type B	0.024
Type D	0.019
Type E	0.027

The calibrated *m* values were validated by running CAESAR-Lisflood on each catchment and comparing the discharge output to the gauge data. The input DEM was clipped to the location of the gauge within the catchment and the model run using the rainfall records of matched dates. The simulation discharge records fell within the same order of magnitude as those measured at the associated gauge, and the distribution of peak discharge values (including outliers) indicates a similar range of values encompassed by each pair of hydrographs (Fig. 5). The distributions measured at the gauges are skewed further to the left than the modelled values, as variations in low flows were lost in CAESAR-Lisflood as the model was parameterised to skip flow and sediment transport calculations below the entrainment threshold.

The hourly rainfall records input to the final model simulations were additionally benchmarked to ensure that the number of geomorphically significant flood events was broadly comparable between the study catchments. The number of events exceeding the 2 year reccurance interval flood discharge (Q_2) was thus established using the model calibration runs, and the rainfall records clipped so that the same number of events were simulated in each catchment. This parameter was selected as a representative flow that readily transports sediment, and which is comparable to bankfull discharge (Hey and Thorne, 1986; e.g. Czuba and Foufoula-Georgiou, 2014; Henshaw et al., 2020). Values for each catchment were estimated using flood frequency analysis on the discharge gauge data and simulated discharge output values. The two datasets produced similar or identical numbers of peak flow events, so the values from the modelled discharge records were used to identify the shortest date range encompassing 10 bankfull flow events. The resulting rainfall record was repeated twice to produce the benchmarked rainfall input. Additionally, one year was identified in each catchment record which included two Q_2 events, and the record for this year was added to the beginning of each input three times to serve as the 'spin-up' period. The subsequent 20-40 year timescale in each catchment thus encompasses a sufficient number of effective events to identify catchment-scale routing patterns, while maintaining reasonable computational runtimes.

Complete and robust parameterisation and validation of catchment-scale landscape evolution models is notoriously difficult in the (common) absence of spatially- and temporally-distributed data on grain size, morphological change and sediment yield. Our aforementioned use of hydrometeorological data from the study catchments was designed to ensure simulated sediment transport and morphodynamic evolution throughout the modelled networks were driven by sufficient flood events of appropriate (geomorphologically-effective) magnitude and comparable frequency. However, other parameters (e.g. initial grain size, vegetation, etc.) were standardised across the study catchments to aid isolation of topological influences, and many (e.g. grid cell size) are necessarily lumped within the model. Our analytical framework does not, therefore, seek to compare simulated sediment yields between study catchments (or, indeed, to their real-world equivalents) in absolute terms, but instead examines how relationships between temporal dynamics in outlet sediment yields and the internal spatio-temporal dynamics of geomorphological change within the study catchments varied according to network type. In this sense, our simulations may be classed as bridging an exploratory and explanatory nature (c.f. Desjardins et al., 2020; Larsen et al. 2014). CAESAR-Lisflood has proven capability in representing geomorphological processes to sufficient degree that broad spatial and temporal patterns of morphological change and sediment yields (or their proxies) can be replicated in a wide range of fluvial environments (e.g. Coulthard and Macklin, 2001; Feeney et al., 2020), while existing conceptual models and empirical studies (e.g. Benda et al., 2004a, 2004b; Benda, 2008; Rice, 2007, Walley et al., 2018) provide a basis against which to evaluate our results.

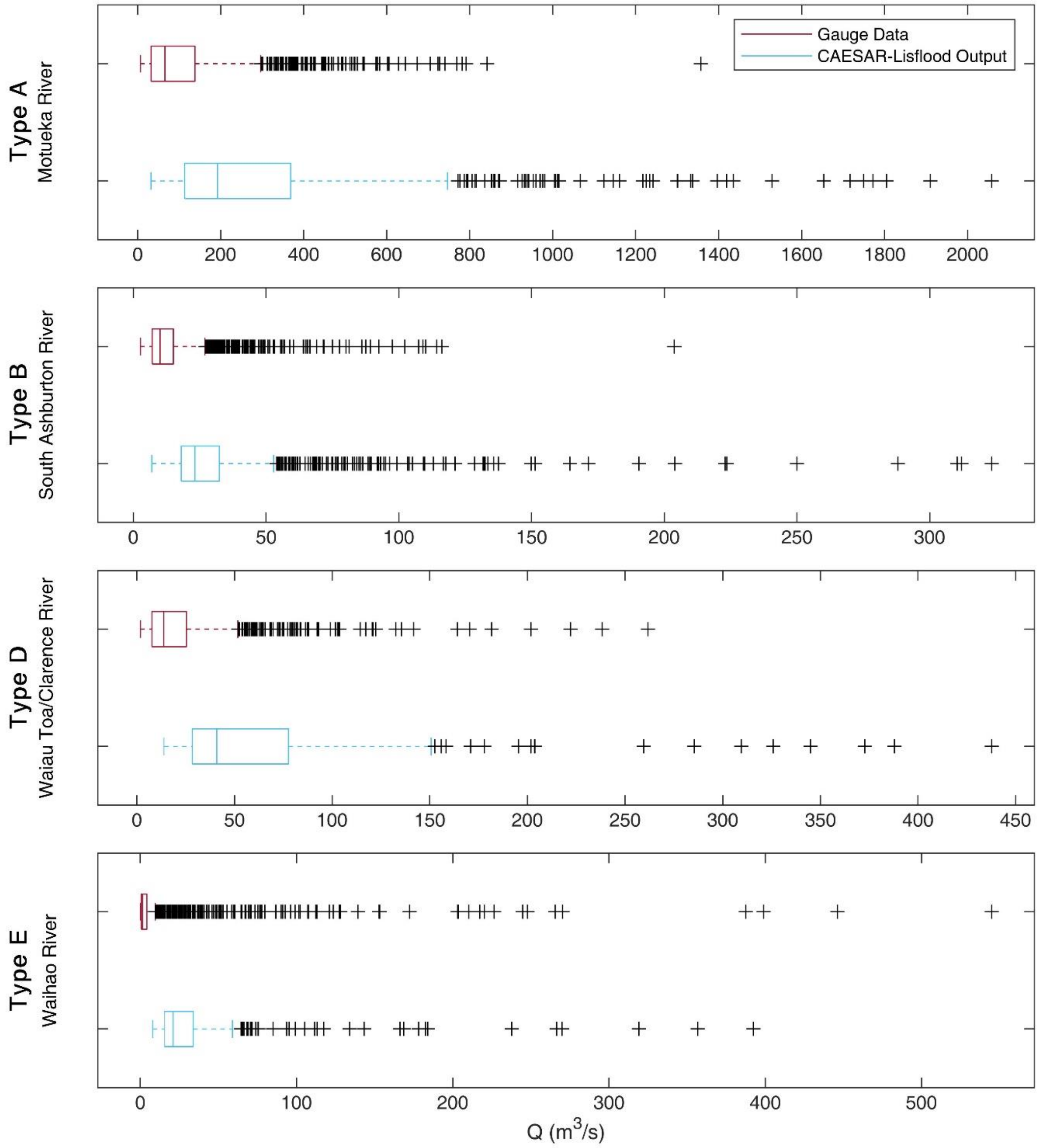

Figure 5. The distribution of peak discharge outputs of the CAESAR-Lisflood model, compared to the peaks from the hydrological gauge data in each study catchment. A similar range of values is encompassed by each pair of hydrographs, although the

discharge measured at each gauge is more left-skewed than those calculated by CAESAR-Lisflood.

3.2 Visualisation of model outputs

Analysing the spatial and temporal patterns of sediment routing across the four study catchments necessitated visualising the results in a comparable manner. The CAESAR-Lisflood model can generate several different raster outputs at user-defined intervals; but grid-based results make it difficult to differentiate the channel network from the bounding hillslopes, and do not easily exhibit the overall behaviour of reaches or tributary junctions. The model was therefore set to save DEM rasters every two months of simulated time, and a method devised for converting the volume of storage change along the channel network into a linear network format (Fig. 6). The river network was thus defined as a set of hierarchically connected 'links', which each represent a segment of the network between two tributary junctions, or between a tributary junction and a source/outlet. The active channel network first had to be defined within the raster grid, which was achieved by generating a buffer around each linear network shapefile with a width three times the grid cell size. This buffer was manually adjusted along the larger valley floors to encompass all change evident in a DEM of Difference calculated for the entire simulation (final DEM output – initial DEM input). It is likely that this method overestimates the width of valley floors in headwater tributaries; however, the amount of change in these zones was observed to be minimal. Once the area was defined, individual cells within the active channel area needed to be assigned to specific links without any overlap at tributary junctions. The linear network was converted into a point cloud and used to generate a Voronoi diagram for the entire catchment, establishing proximity-based boundaries between each link which were applied to the network buffer. The buffer was then converted into raster format using the same cell mapping as the original DEM, thus defining sets of cells as 'links' which could be applied to the output rasters.

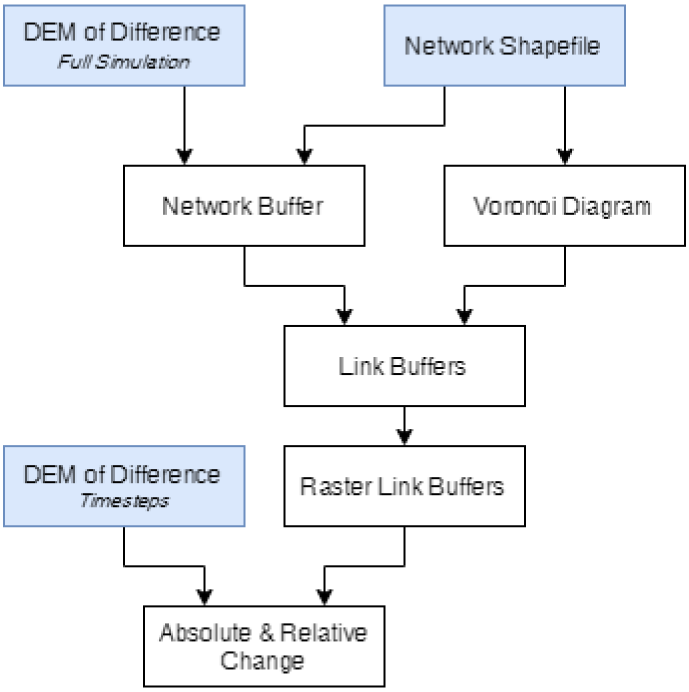

Figure 6. Method for extracting link values of absolute and relative change for each timestep.

Using MATLAB, a DEM of Difference was calculated for each timestep, by taking the output DEM and subtracting the one from the previous timestep. The change in elevation was converted to change in volume by multiplying the resulting raster by cell area, and the defined buffer zones used to calculate link-based values. The sum of all values in each link calculated the *relative* change, producing positive values representing aggradation and negative values representing erosion. The sum of the absolute values calculated *absolute* change, generating values which represent the total volume of change in that link, regardless of direction. In addition to producing linear maps, extracting the absolute and relative change in each link thus provides a basis for classifying link behaviour. Links with high values in both variables, whether the relative change is positive or negative, indicate locations in the network acting as sinks or sources, respectively. Similarly, links with high absolute change and a value of relative change near zero likely behave as exchange reaches, exhibiting dynamic behaviour but little net aggradation or erosion.

4. CATCHMENT-SCALE PATTERNS OF SEDIMENT TRANSFER

4.1 Spatial patterns of sediment flux

The CAESAR-Lisflood results from each of the four study catchments exhibit distinctly different patterns of dynamic behaviour. Figure 7 displays the total absolute change and total relative change in the most dynamic links over the course of each simulation, with key hotspots labelled for ease of identification. In the Type A catchment, the most dynamic reaches are concentrated in the lowest 5th order reach and the connected 4th order tributaries, with some extending into 3rd order links (Fig. 7a). These links exhibit largely erosional behaviour over the course of the simulation, with some intermittent aggradational zones. Key hotspots occur at confluence 4 at the head of the 5th order reach, and link 2 just downstream. This pattern is indicative of the dissected network structure, in which confluence 4 represents a significant point of convergence. Hotspots 3 and 6 appear to behave differently to the other identified locations as they indicate highly aggradational links, which occur at the outlet of subnetworks relatively disconnected from the primary sediment pathways.

The dissected Type B network contains a similar spatial pattern to the Type A catchment, in which the most dynamic reaches are also concentrated within the 5th order reach, extending from the outlet to confluence 2 (Fig. 7b). Sediment is concentrated at points in the network where tributaries of similar magnitudes converge, although the values of absolute change are more evenly distributed across the catchment with fewer significant hotspots. A similar pattern emerges from the values of relative change (Fig. 7f), with the links indicating erosion and deposition exhibiting values closer to -1 and 1, respectively, compared to those in the Type A network. These patterns suggest that sediment moves more readily through the Type B catchment and may therefore be more sensitive to disturbance events, with the identified hotspots possibly having a lesser impact on the overall pattern of sediment connectivity.

In contrast to the Type A and B catchments, the Type D river is large, elongate, and contains a network oriented around a central mainstem. The spatial pattern of dynamic reaches occurs predominantly through this mainstem channel, but also extends upstream of location 2 into the headwater tributaries (Fig. 7c). This confluence is both a significant point of convergence in the network, and a drainage anomaly in which the tributaries converge at an angle greater than 90°, and subsequently exhibits a value of absolute change significantly higher than anywhere else in the catchment. The map of relative change indicates that hotspot 2 is a highly aggradational set of links (Fig. 7g), and it is therefore likely that this site intercepts sediment from the upstream network and modulates its delivery downstream. The downstream pattern of relative change then suggests that transport through the mainstem channel is intermittent, with alternating aggradational and erosional links. This pattern is particularly emphasised at hotspot 2, which indicates a zone of aggradation immediately upstream of a gorge.

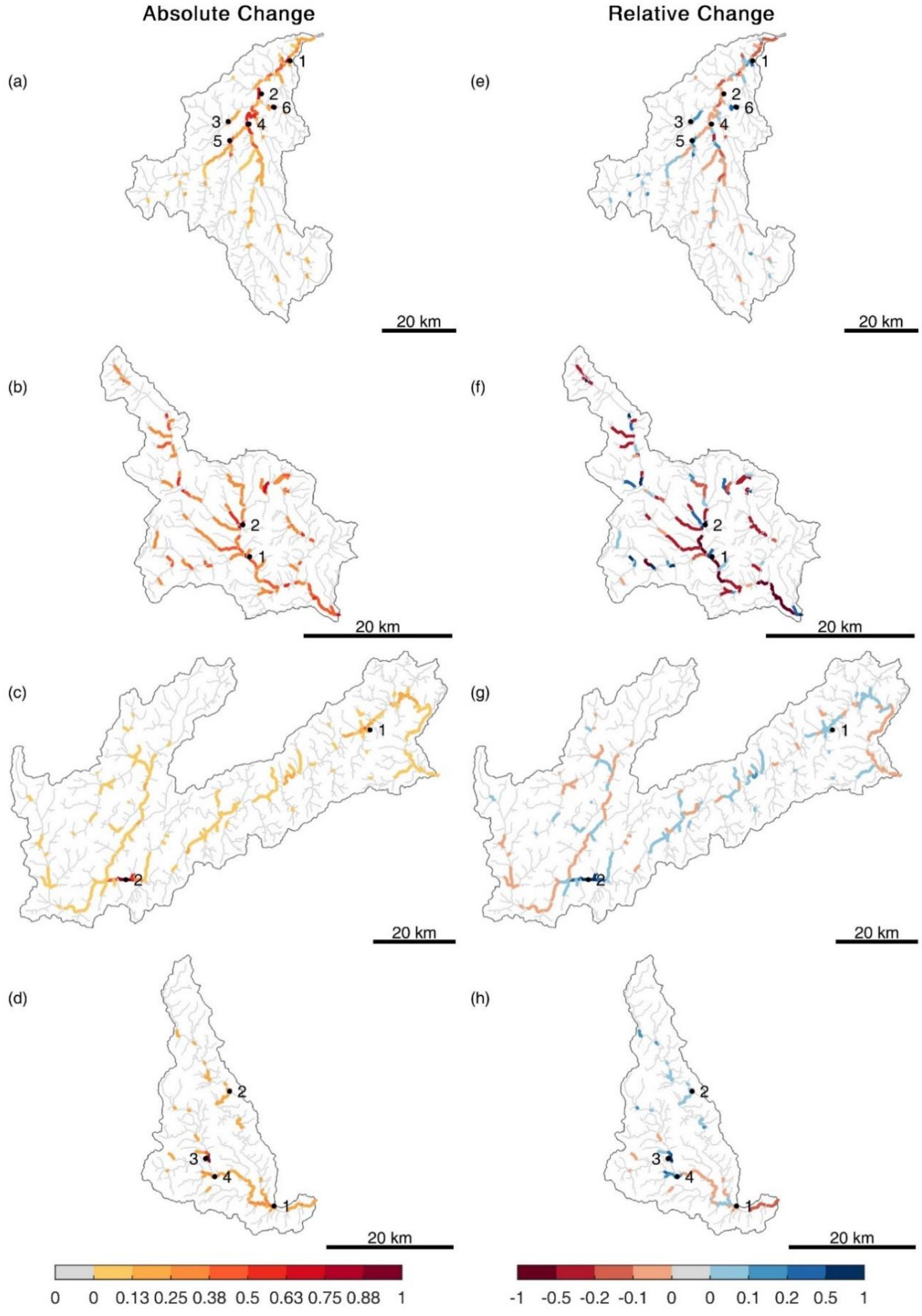

Figure 7. Simulation results for the Type A (a & e), Type B (b & f), Type D (c & g) and the Type E catchments (d & h). Panels (a-d) show the absolute change calculated from the CAESAR-Lisflood outputs, and panels (e-h) show the relative change in each link. Values of absolute change are normalised by the maximum value of each dataset, thus a value of 1 in different catchments does not indicate the same volume of change. Relative change is divided into net aggradation (positive) and net degradation (negative), and the values

are normalised by the largest absolute value of each dataset, thus a value of 1 and -1 in the same catchment indicates the same volume of change. The links identified as the most dynamic (panels a-d) are used to identify which links to highlight in the maps of relative change (panels e-h).

The Type E network has a similarly mainstem-dominant structure but is split between two key subcatchments which converge at location 1 (Fig. 7d). This confluence thus represents a significant point of convergence in the network and consequently exhibits dynamic behaviour like those in the other catchment types. The western subcatchment upstream of hotspot 1 appears to be more dynamic than the eastern network, with high values of absolute change concentrated through the central mainstem up to hotspot 4. The pattern of relative change through this reach suggests a somewhat intermittent pattern of transport (Fig. 7h), similar to behaviour in the Type D mainstem. Location 3 is the most dynamic links in the network however, which occurs just upstream of hotspot 4 separated by a highly confined reach. This location accumulates sediment transported from the small subnetwork upstream, likely in response to the controlling influence of the downstream link, and thus exhibits similarities to hotspots 3 and 6 in the Type A network.

4.2 Temporal patterns of sediment flux

The simulation results were divided into annual timesteps to explore how the observed spatial patterns of absolute and relative change evolve over time. A key observation which emerged from these maps was the frequent dissimilarity between sequential timesteps, where the overall pattern of dynamic links does not appear to be influenced by the pattern observed in the previous timestep. Instead, years which exhibit similar values of absolute change summed across all links in the network display clear similarities in spatial patterns. Two animation files are thus provided for each catchment comprised of maps of absolute and relative change for each timestep in the simulation, one ordered by timestep and the other by the total volume of absolute change in each year.

The spatial patterns of absolute change in the Type A catchment are dynamic, with hotspot links occurring at different locations across the simulation (Animation A.1). The dissected network structure results in sediment transport concentrating in multiple subnetworks, and the Type A network thus exhibits the most hotspots out of the four study catchments. These hotspots occur at key junctions in the network and do not move over time, although some hotspots do not exhibit dynamic behaviour in every timestep. Hotspot 4 emerges as one of the most dynamic links in the network, as there are very few timesteps in which it is not highlighted. The comparatively low values of relative change indicate that sediment is regularly deposited and re-entrained at this confluence, thus modulating the transfer of sediment through the downstream reaches.

The relationship between total absolute change and the spatial patterns of dynamic links is displayed in Animation A.2, which exhibits the Type A annual timesteps in order of magnitude. The most active timesteps (1-4) indicate spatial patterns concentrated in the downstream parts of the catchment and hotspots at key confluences, suggesting that the entire catchment is readily transporting sediment. With less activity, the overall pattern of the most dynamic reaches shifts away from the main valley floor and hotspots occur further upstream (e.g. timesteps 6 and 5, 29 and 16), exhibiting variability in the pattern of transport across the subnetworks. With further decreases, hotspots and the most dynamic links move into the upper, steepest parts of the catchment (e.g. timesteps 14 & 24), before the volumes of change across the dynamic links become similar enough across the steep slopes that no hotspots are apparent (e.g. timesteps 30 & 25). At this point, sediment transport is likely governed by hillslopes rather than fluvial processes. This relationship between the spatial pattern of dynamic links and total absolute change in the Type A catchment thus suggests that sediment transport in separate subnetworks activates under different conditions, and that the amount of change occurring within each subcatchment tends to be highlighted at each outlet.

Animation A.1. Annual Timesteps of absolute and relative change for the Type A catchment (Motueka River). Timesteps are displayed in sequential order.

Animation A.2. Annual Timesteps of absolute and relative change for the Type A catchment (Motueka River). Timesteps are displayed in order of descending magnitude of absolute change.

The spatial pattern of absolute change in the Type B network is the most dynamic of the study catchments, with little overall similarity between timesteps and various emerging hotspots (Animation B.1). The pattern of dynamic links which emerges across the network is inconsistent throughout the simulation and exhibits greater diversity than identified in the maps of all timesteps. Hotspots move within the network over time, and typically occur within the wide, flat parts of the central catchment rather than the downstream 5th order reaches. Like the Type A river, the Type B catchment exhibits similarity in the distribution of dynamic links at timesteps which have similar volumes of total absolute change, although the majority of timesteps exhibit low values (Animation B.2). Of the few timesteps which have larger volumes of total absolute change, only a few have values similar enough to exhibit consistency between the spatial patterns of dynamic links (timesteps 5, 13), although the relationship is clearly evident in the low-value timesteps (e.g. 4, 6, 7, 8). These again occur in some of the steepest parts of the catchment and indicate aggradational behaviour from hillslopes.

Animation B.1. Annual Timesteps of absolute and relative change for the Type B catchment (South Ashburton River). Timesteps are displayed in sequential order.

Animation B.2. Annual Timesteps of absolute and relative change for the Type B catchment (South Ashburton River). Timesteps are displayed in order of descending magnitude of absolute change.

The spatial pattern of absolute change in the Type D network is the least dynamic of the study catchments, as the distribution of dynamic links across the network remains very similar throughout the simulation (Animation D.1). The pattern is consequently very similar to the previously presented maps of the full simulation (Fig. 7), and the identified hotspot at confluence 2 exhibits the most dynamic behaviour in all timesteps except those with the least volumes of total absolute change. The consistency does not extend to the patterns of relative change, although the collection of links at location 2 indicate predominantly aggradational behaviour throughout the simulation. Given this more consistent spatial pattern in the Type D catchment, a relationship between the distribution of dynamic links and the volume of total absolute change is difficult to determine at the larger volumes (e.g. Animation D.2, timesteps 13, 5, 4, 26). Figure 8 indicates that the spatial pattern is more consistent over a large range of absolute change values than the Type A and B networks, but exhibits the same shift in spatial pattern in timesteps of little total absolute change. With decreasing volumes, the dynamic behaviour moves upstream (e.g. Animation D.2, timesteps 11 and 18) and becomes consistently aggradational regardless of the sequential order of the timesteps (e.g. Animation D.2, timesteps 22 and 24), and these patterns likely reflect the shift from fluvial transport to hillslope processes.

Animation D.1. Annual Timesteps of absolute and relative change for the Type D catchment (Waiau Toa/Clarence River). Timesteps are displayed in sequential order.

Animation D.2. Annual Timesteps of absolute and relative change for the Type D catchment (Waiau Toa/Clarence River). Timesteps are displayed in order of descending magnitude of absolute change.

The spatial pattern of absolute change in the Type E catchment is less dynamic than the Type A or B networks, but also indicates less consistency over time than the Type D river (Animation E.1). The locations of key reaches appear to correspond with those highlighted in the previous maps of the full simulation results (Fig. 7), and the western subcatchment remains more consistent than the east throughout the simulation. Hotspot 3 consistently acts as an aggradational sink, likely influencing the predominantly erosional behaviour of the downstream reaches, while hotspot 2 exhibits intermittent transport through a collection of reaches. As in the Type D network, hotspot 1 lies at the junction of two key subnetworks and acts as a bottleneck modulating connectivity downstream, although this confluence occurs closer to the outlet and thus does not have the same impact on the overall pattern of connectivity. Despite this relatively consistent spatial pattern of dynamic links it is clear that timesteps with similar volumes of absolute change exhibit similar spatial patterns within the network (e.g. Animation E.2, timesteps 4 and 12, 6 and

7). The most active timesteps (1, 2, 3, & 4) exhibit the most dynamic behaviour in the lower reaches of the network, suggesting transport throughout the catchment. As activity decreases, the most dynamic reaches move upstream (e.g. Animation E.2, timesteps 12 and 18) and into the steeper parts of the catchment (e.g. Animation E.2, timesteps 8 and 6), reflecting the same trend of distributed sediment transport observed in the other catchments. Those timesteps with very low volumes of total absolute change again exhibit nearly identical patterns of aggradation within the steepest tributaries (e.g. Animation E.2, timesteps 33 and 16), driven by a shift from fluvial processes to into hillslopes.

Animation E.1. Annual Timesteps of absolute and relative change for the Type E catchment (Waihao River). Timesteps are displayed in sequential order.

Animation E.2. Annual Timesteps of absolute and relative change for the Type E catchment (Waihao River). Timesteps are displayed in order of descending magnitude of absolute change.

In every study catchment there is a clear relationship between the distribution of dynamic links across the network and the total absolute change occurring in each timestep. Timesteps with similar values of change produce similar patterns of dynamic links irrespective of the simulation sequence, a pattern most pronounced in years with little total change. There appears to be greater consistency in the spatial patterns in the Type D and E catchments; however, each simulation also contains variable proportions of timesteps with high values of total absolute change compared to low ones. Figure 8 therefore compares this relationship across the network 'types', in which panel (a) displays the total absolute change in each timestep sorted by magnitude, and panel (b) indicates the spatial patterns of dynamic links associated with those change values. These figures indicate that while the four network 'types' do have distinctly different distributions of total absolute change values over time (Fig. 8a), those distributions do not correspond to a similar diversity in spatial patterns of dynamic links (Fig. 8b) supporting the greater consistency observed in the Type D and E animation maps. This relationship is particularly evident in the Type D network which has a much higher proportion of timesteps with high values of total absolute change compared to the other network 'types' (Fig. 8a), but a lower proportion of distinct spatial patterns of active links (Fig. 8b).

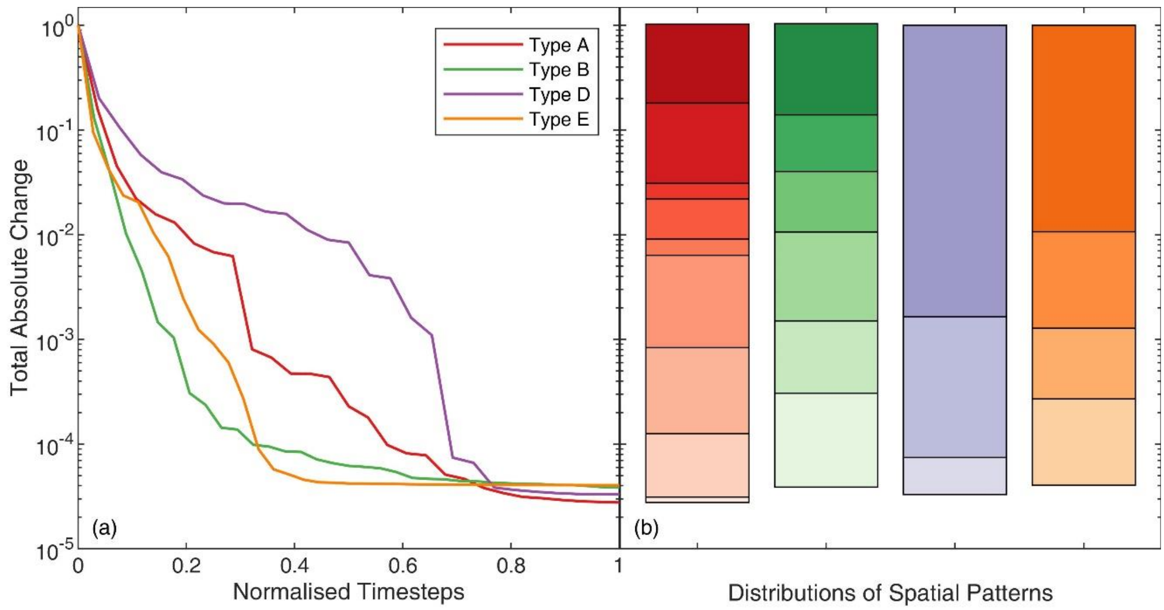

Figure 8. Distributions of total absolute change in each study catchment, with (a) timesteps sorted by magnitude of change and (b) the distributions of distinctive active reach combinations across the values of total absolute change. Values of absolute change are normalised by the largest value in each simulation, and the timesteps in (a) are normalised by the length of each simulation.

4.3 Outlet Relationships

The relationship between the spatial pattern of dynamic links and the magnitude of network-scale change can be further explored through the processes of sediment and flow discharge at the outlet. These are likely to be the primary drivers of total absolute change, and the strength of the relationships provide insight to the network's connectivity. The CAESAR-Lisflood model does not record flow or sediment discharge throughout the catchment, so Spearman's correlation matrices were generated from the annual values at the outlet. Table 4 displays the correlation coefficients in which insignificant relationships ($p > 0.05$) are greyed out.

Table 4. Correlation coefficients of the relationships between total absolute change (CHa), sediment discharge (Qs) and flow discharge (Qw). Values with statistically insignificant relationships ($p > 0.05$) are greyed out.

	Type A	**Type B**	**Type D**	**Type E**
CHa and Qs	0.98	0.11	0.79	0.95
CHa and Qw	0.17	0.32	0.51	0.84
Qw and Qs	0.20	0.57	0.45	0.93

The Type A catchment exhibits a strong, positive relationship between the total absolute change and sediment discharge at the outlet, but no significant relationships between the other variables. This pattern suggests that the volume of sediment reaching the outlet is proportionate to the volume of sediment moving within the network, and thus the volume of absolute change in each timestep is largely driven by processes of sediment transport. These variables are not related to flow discharge, however, which indicates that the sediment transport and absolute change processes are disconnected from flow magnitude. These relationships thus indicate a disconnected catchment, in which sediment stores within the network prevent sediment transport in proportion to flow discharge.

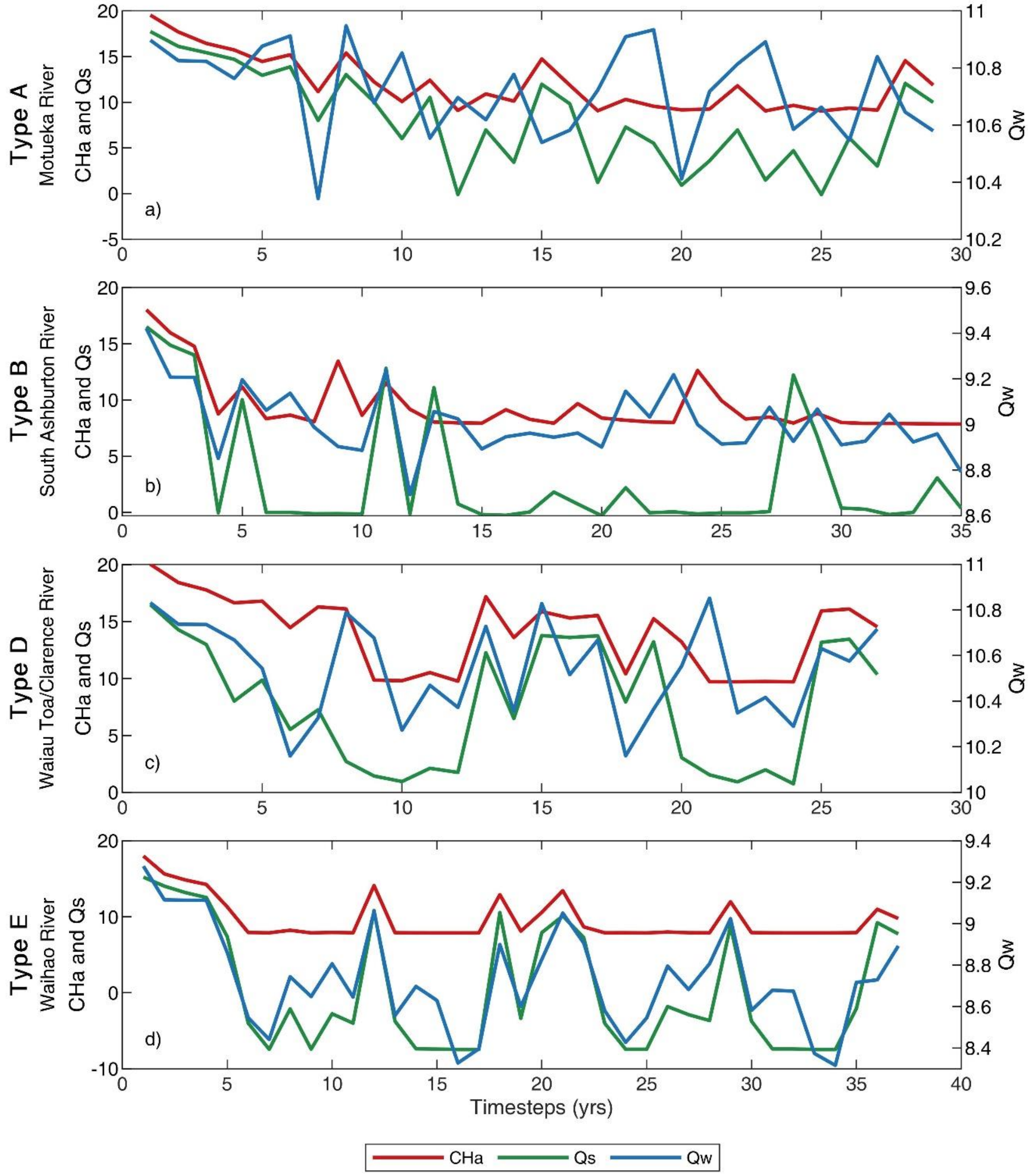

Figure 9. Annual timeseries data from the outlets of the four model catchments, with absolute change (CHa), sediment discharge (Qs) and flow discharge (Qw) plotted over time.

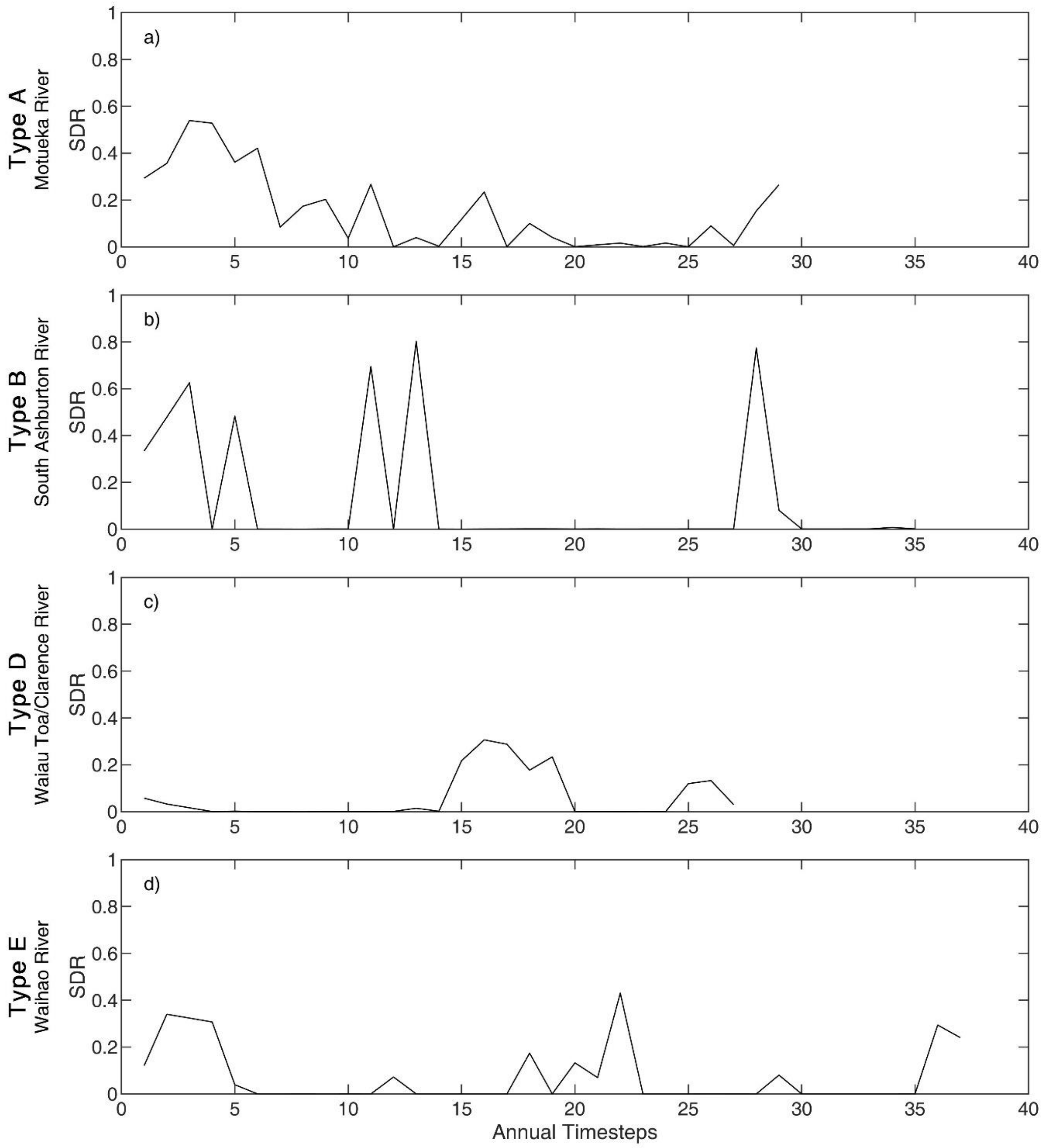

Figure 10. Sediment delivery ratios in each catchment, calculated as the ratio of annual sediment yield at the outlet to annual erosion across the catchment.

In contrast to the Type A catchment, the Type B network does not display significant relationships between total absolute change and either of the other variables, but contains a significant, moderate relationship between sediment and flow discharge (Table 4). This pattern suggests that the network contains relatively few perturbations which modulate the sediment signal, and that geomorphic change occurs across a range of flow conditions which are not always conveyed to the outlet. These relationships thus indicate that the Type B network is more connected than Type A, as high flows transport larger volumes of sediment more consistently, but the relatively weak relationship and non-linear correlation with total absolute change indicate the catchment is still largely disconnected. As in the Type A catchment, sediment is likely being trapped by internal stores and thus not transported to the outlet, although Figs. 9b and 10b suggest this transfer occurs much more efficiently during peak flows.

The Type D catchment exhibits significant, moderate relationships between all three variables, with a slightly stronger correlation between total absolute change and sediment discharge at the outlet (Table 4). As in the Type A network, this suggests that the volume of sediment reaching the outlet is relatively proportionate to the volume of sediment moving in the network, and that the volume of absolute change in each timestep is driven by sediment transport processes. Unlike the Type A catchment, however, both total absolute change and sediment discharge exhibit moderate correlations with flow discharge, indicating greater connectivity within the catchment overall. The moderate relationship between flow and sediment discharge displays variable sediment volumes within both high and low flow discharges, suggesting some disconnectivity within the network. As previously observed, this is likely to be the modulating influence of the hotspot at location 2 at the head of the mainstem reach, which acts as a bottleneck preventing sediment transport readily downstream and impeding stronger relationships between flow discharge and the other variables.

The Type E catchment exhibits significant, strong relationships across all three variables, indicating that sediment transfer is more connected than any of the other catchments (Table 4). High flow conditions drive high sediment discharge and geomorphic change across the network, and these values decrease steadily with flow magnitude. As in the Type B catchment, the Type E network exhibits skewed distributions of total absolute change and sediment discharge, indicating a low-energy river which often operates in baseflow conditions. This has not impacted the strength of the relationships as much as in the Type B network, however, despite being particularly pronounced in the two distinct groupings within the sediment discharge data. These groups appear to be associated with high and low flow conditions with no values occurring in between, suggesting that some disconnectivity likely occurs under very low flow conditions.

The outlet relationships from the study catchments thus exhibit relatively strong relationships in the Type D and E networks, and comparatively weak ones in the Type A and B catchments. The non-linear relationships exhibited by Types A and B are characteristic of fluvial systems, in which high flow conditions may induce erosional or aggradational behaviour of varying magnitude. In contrast, the Type D and E catchments exhibit relatively linear relationships, which do not result from the model functionality as CAESAR has been established to enable self-organised criticality (SOC) and thus non-linear behaviour (Coulthard and Van De Wiel, 2007). This same study identified catchment morphology as the most significant driver of non-linearity in fluvial systems due to the varying potential for internal sediment storage (Coulthard and Van De Wiel, 2007); and Walley et al. (2018) identified a greater potential for storage in a dissected river network compared to a mainstem-dominant structure, resulting from an increased number of confluences at which similar-sized tributaries converged. These studies, combined with the disparity in outlet relationships identified using the CAESAR-Lisflood model suggest that sediment pathways through mainstem-dominant networks are fundamentally different to those in their dissected counterparts, and exhibit greater connectivity over a variety of flow conditions.

5. DISCUSSION

The key differences in the spatio-temporal patterns of sediment connectivity between catchments with divergent network structures are summarised in Fig. 11, within the framework of the original topological classification outlined in Walley et al. (2020). Most of the variation in sediment connectivity occurs between the dissected networks (Type A and B) compared to the mainstem-dominant structures (Type D and E), which corresponds to the first component of the PCA (horizontal axis) and thus the greatest variation in the original topological metrics. This is evident in the spatial patterns of dynamic links, which indicate that change occurs throughout the Type A and B networks but concentrates in the central channels of the mainstem-dominant catchments. These patterns correspond to the distribution of hotspots in the different network structures, as the nature of convergence in the Type D and E catchments generates hotspots further upstream compared to the Type A and B networks. The two hotspots identified in the Type D catchment appear to have the most significant influence on sediment routing, particularly in comparison to the relatively insignificant hotspots in Type B. This suggests that the impact of these hotspots on modulating sediment routing is additionally influenced by network topography (vertical axis).

The differences observed in the temporal patterns of sediment connectivity exhibit similar variation, with most occurring along the first principal component. This is evidenced by the spatial pattern of dynamic links evolving more readily over time in dissected network structures, and key differences in the relationships between drivers of change in each catchment. These results suggest that the Type B network exhibits the most dynamic behaviour, in direct contrast to the Type D catchment which appears to contain the most stable pattern of dynamic links. These patterns were found to correspond to the total absolute change occurring in each annual timestep, and while this relationship was evident in all network types, the pattern of dynamic links adjusted to variation in total absolute change more readily in the dissected catchments. This trend is likely driven by the relationships between total absolute change, flow, and sediment discharge, which were also found to be influenced by network structure. The mainstem-dominant networks exhibit much stronger, linear relationships between these variables, while those in the dissected networks are non-linear.

The patterns of sediment connectivity observed in the model results exhibit a clear relationship between sediment routing and network structure and support several conceptual models of catchment-scale connectivity. Few studies explicitly explore this relationship, and of these, only Walley et al. (2018) systematically analyses the role of network structure in modulating the downstream transfer of sediment. In both studies, the dissected structure drives greater interaction between sediment stores at tributary confluences compared to the mainstem-dominant network, which exhibits transfer predominantly along the central 'root' channel (Walley et al., 2018). In addition, the primary hotspot identified in the dissected network of the Walley et al. (2018) study occurs close to the outlet, similar to the Type A network, much further downstream than the mainstem-dominant structures (e.g. Type D) which occur at the head of the mainstem reaches. These results further support the conceptual model of catchment-scale connectivity posed by Benda et al (2004a, 2004b), Benda (2008) and later quantified by Rice (2017), which defines significant confluences as tributary junctions that exhibit substantial changes in channel and valley morphology. They suggest that such confluences are likely to occur throughout the network and with greater frequency in compact (dissected) catchments compared to linear (mainstem-dominated) structures because they have a higher probability of relatively large tributaries joining the network downstream (Benda et al., 2004a; Rice, 2017). These patterns suggest that some tributary junctions are topologically predisposed to confluence effects and correspond to the distributions of hotspots observed in the modelled catchments.

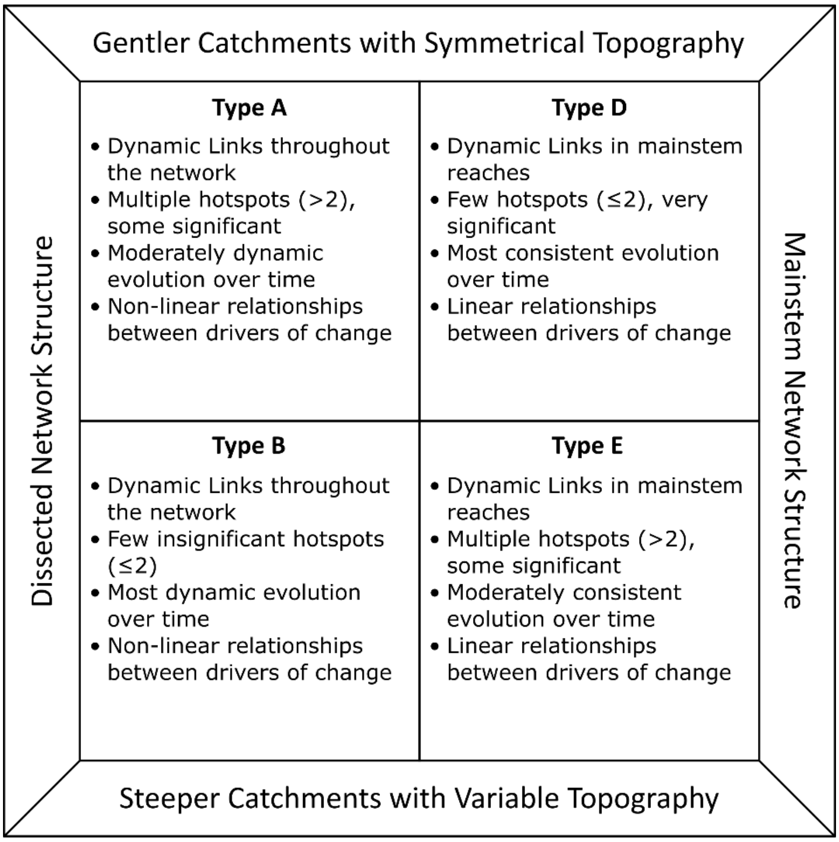

Figure 11. Conceptual model of the spatio-temporal patterns of sediment connectivity within the topological classification framework.

Unlike previous catchment-scale sediment dynamics studies, numerical modelling offers a unique opportunity to capture dynamical sediment routing behaviour at the catchment scale. LEMs like CAESAR-Lisflood employ DEMs at fine resolutions to model highly detailed processes and complex outcomes. They are readily amenable to scenario modelling and have robust uncertainty analyses, but are also computationally intensive, and arguably over parameterised for process-specific studies. A key drawback in using the CAESAR-Lisflood model was the inability to track the pathways of individual sediment parcels through the fluvial network, as there is no way to extract this information at the catchment scale from the cellular approach to sediment routing. This grid-based structure also distributes the computational processing across the entire catchment rather than concentrating it on the key changes within fluvial channel network, and severely limited our ability to explore sediment routing across different grain size fractions. Alternative vector-based models have more recently become more prominent in modelling catchment-scale sediment dynamics to address some of these shortcomings (e.g. the network-based framework (Czuba and Foufoula-Georgiou, 2014, 2015), CASCADE (Schmitt et al., 2016; Tangi et al., 2019)), and may provide better fit-for-purpose solutions. Rather than attempting to model every aspect of the fluvial system, these models focus on simulating individual processes to limit the necessary computational capabilities without over-simplifying the system.

The topological control of river networks on catchment-scale sediment dynamics has significant implications for our understanding of fluvial systems, river management and future research opportunities. Knowledge of the discontinuous transfer of sediment is important for minimising the impact of a variety of activities, including mineral and gravel mining, channelisation and flood protection schemes and the management of hydro-power dams. The role of hotspots in sediment connectivity also has implications for estimating the spatial and temporal responses to disturbance events, and the potential downstream impacts of landslide dams, aggradation and channel avulsion, and habitat degradation. Understanding the spatial and temporal behaviour of hotspots in different network types also has significant implications for our understanding of sedimentary records, and interpretations of paleoenvironmental reconstruction based on stratigraphy. Models of landscape evolution tend to simulate environmental signals as dampened by the transport system or lagged, but it has been suggested that this may be too simplistic (Coulthard and Van De Wiel, 2007; Jerolmack and Paola, 2010). Jerolmack and Paola (2010) instead propose that non-linearity and self-criticality in fluvial systems can destroy environmental signals transported through fluvial systems by 'shredding', thus making interpretations of paleoenvironmental conditions from sedimentary records problematic (Coulthard and Van De Wiel, 2007; Jerolmack and Paola, 2010). The patterns of sediment routing identified in this study support the idea that fluvial systems extensively modulate sedimentary inputs, but further indicate that dissected catchment structures transform environmental signals more substantially than others. This has significant implications for research involving sedimentary records, as it suggests that system memory is better preserved in catchments with mainstem-dominant structures, and thus the stratigraphy observed in these networks is more likely to reflect the paleoenvironmental conditions than internal system dynamics. The scale of such networks must also be considered as particularly large rivers will likely incorporate a variety of internal structures, especially if the catchment area extends into disparate regional environments. Further research is required into these relationships; however, it is clear that the influence of network structure on the spatio-temporal patterns of sediment connectivity is vital for our understanding of fluvial systems at the catchment scale.

6. CONCLUSIONS

Drainage network topology plays a clear role in modulating the spatio-temporal pattern of sediment transfer from source to sink. Building on the theoretical understanding of how sediment is transferred through catchment-scale river systems and the analysis of network topology provided by Walley et al. (2020), this study compares patterns of sediment routing across topologically distinct structures, and identifies key differences in the spatio-temporal patterns of sediment transfer. These patterns indicate that dynamic behaviour is structured differently in each of the network 'types', with particular divergence between the dissected networks (Type A and B) which exhibit dynamic links throughout the network, and the mainstem-dominant structures (Type D and E) which indicate that change is concentrated within the mainstem reach. Key differences were also observed in the occurrence of hotspots across the networks, with the greatest dissimilarity between the patterns was observed between the Type B network which contained several insignificant hotspots, and the Type D structure, in which a single site significantly influenced the overall pattern of connectivity. These distributions likely influence the observed temporal patterns of sediment connectivity, which exhibit similar variation between the most consistent patterns in the Type D network compared to the most inconsistent in the Type B catchment.

Control of network topology on sediment routing and connectivity is further evidenced by the different relationships between absolute change and flow and sediment discharge at the outlet of each network. The dissected networks (Type A and B) exhibit mostly non-linear relationships between these variables in contrast to the moderate-strong linear relationships in the mainstem-dominant structures, suggesting that the latter exhibit greater connectivity across a range of flow conditions. This difference has significant implications for our understanding of sedimentary records and interpretations of paleoenvironmental reconstruction based on stratigraphy, as it suggests that the extent of transformation of environmental signals through fluvial systems is largely dependent on network structure. Further research is necessary to fully understand how such signals are modulated by network topology and interaction with hotspots, particularly the internal transformations not captured by the CAESAR-Lisflood model.

ACKNOWLEDGEMENTS

The authors would like to thank the Otago Regional Council, Environment Canterbury and NIWA for supplying hydrological gauge data. This study was supported by funding from a Principal's Studentship at Queen Mary, University of London. The authors declare that they have no conflict of interest.

AUTHOR CONTRIBUTIONS

Y. Walley conceived of the presented idea, which was then developed and planned by both authors. Y. Walley carried out the data acquisition, simulations and subsequent analysis, supervised and assisted by A. Henshaw. Y. Walley wrote the original draft of the manuscript, which was then developed and edited by both authors.

DATA AVAILABILITY STATEMENT

The data sets used and/or analysed during the current study are available from the corresponding author on reasonable request.

REFERENCES

Benda, L., 2008. *Confluence environments at the scale of river networks*, in: Rice, S.P., Roy, A., Rhoads, B.L. (Eds.), River Confluences, Tributaries and the Fluvial Network. Wiley & Sons Ltd., Chichester, UK, pp. 271–300.

Benda, L., Andras, K., Miller, D.J., Bigelow, P.E., 2004a. *Confluence effects in rivers: Interactions of basin scale, network geometry, and disturbance regimes*. Water Resour. Res. 40. https://doi.org/10.1029/2003WR002583

Benda, L., Poff, N.L., Miller, D.J., Dunne, T., Reeves, G.H., Pess, G., Pollock, M., 2004b. *The Network Dynamics Hypothesis: How Channel Networks Structure Riverine Habitats*. Bioscience 54, 413–427. https://doi.org/10.1641/0006-3568(2004)054[0413:TNDHHC]2.0.CO;2

Beven, K.J., 1997. *TOPMODEL: A critique*. Hydrol. Process. 11, 1069–1085. https://doi.org/10.1002/(SICI)1099-1085(199707)11:9<1069::AID-HYP545>3.0.CO;2-O

Beven, K.J., Kirkby, M.J., 1979. *A physically based, variable contributing area model of basin hydrology*. Hydrol. Sci. Bull. 24, 43–69. https://doi.org/10.1080/02626667909491834

Bracken, L. J., Turnbull, L., Wainwright, J., & Bogaart, P. (2015). Sediment connectivity: a framework for understanding sediment transfer at multiple scales. Earth Surface Processes and Landforms, 40(2), 177-188.

Brierley, G. J., & Fryirs, K. A. (Eds.). (2004). *Geomorphology and River Management*. Blackwell Publishing. https://doi.org/10.1002/9780470751367

Brierley, G., Fryirs, K., & Jain, V. (2006). Landscape connectivity: the geographic basis of geomorphic applications. Area, 38(2), 165-174.

Burt, T. P., & Allison, R. J. (Eds.). (2010). *Sediment Cascades: An Integrated Approach*. John Wiley & Sons, Ltd. https://doi.org/10.1002/9780470682876

Castelltort, S., Goren, L., Willett, S.D., Champagnac, J.-D., Herman, F., Braun, J., 2012. *River drainage patterns in the New Zealand Alps primarily controlled by plate tectonic strain*. Nat. Geosci. 5, 744–748. https://doi.org/10.1038/ngeo1582

Church, M., Kellerhals, R., 1978. *On the statistics of grain size variation along a gravel river*. Can. J. Earth Sci. 15, 1151–1160.

Coulthard, T.J., Kirkby, M.J., Macklin, M.G., 2000. *Modelling geomorphic response to environmental change in an upland catchment*. Hydrol. Process. 14, 2031–2045. https://doi.org/10.1002/1099-1085(20000815/30)14:11/12<2031::AID-HYP53>3.0.CO;2-G

Coulthard, T.J., Lewin, J., Macklin, M.G., 2005. *Modelling differential catchment response to environmental change*. Geomorphology 69, 222–241. https://doi.org/10.1016/j.geomorph.2005.01.008

Coulthard, T.J., Macklin, M.G., Kirkby, M.J., 2002. *A cellular model of Holocene upland river basin and alluvial fan evolution*. Earth Surf. Process. Landforms 27, 269–288. https://doi.org/10.1002/esp.318

Coulthard, T.J., Neal, J.C., Bates, P.D., Ramirez, J., de Almeida, G.A.M., Hancock, G.R., 2013. *Integrating the LISFLOOD-FP 2D hydrodynamic model with the CAESAR model: Implications for modelling landscape evolution*. Earth Surf. Process. Landforms 38, 1897–1906. https://doi.org/10.1002/esp.3478

Coulthard, T. J., & Macklin, M. G. (2003). Modeling long-term contamination in river systems from historical metal mining. *Geology*, *31*(5), 451–454. https://doi.org/10.1130/0091-7613(2003)031<0451:MLCIRS>2.0.CO;2

Coulthard, T. J., & Macklin, M. G. (2001). How sensitive are river systems to climate and land-use changes? A model-based evaluation. *Journal of Quaternary Science*, *16*(4), 347–351. https://doi.org/10.1002/JQS.604

Coulthard, T.J., Skinner, C.J., 2016. *The sensitivity of landscape evolution models to spatial and temporal rainfall resolution*. Earth Surf. Dyn. 4, 757–771. https://doi.org/10.5194/esurf-4-757-2016

Coulthard, T.J., Van De Wiel, M.J., 2007. *Quantifying fluvial non linearity and finding self organized criticality? Insights from simulations of river basin evolution*. Geomorphology 91, 216–235. https://doi.org/10.1016/j.geomorph.2007.04.011

Czuba, J.A., Foufoula-Georgiou, E., 2015. *Dynamic connectivity in a fluvial network for identifying hotspots of geomorphic change*. Water Resour. Res. 51, 1401–1421. https://doi.org/10.1002/2015WR016967.

Czuba, J.A., Foufoula-Georgiou, E., 2014. *A network-based framework for identifying potential synchronizations and amplifications of sediment delivery in river basins*. Water Resour. Res. 50, 3826–3851. https://doi.org/10.1002/2013WR014227

Dawson, M., 1988. *Sediment Size Variation in a Braided Reach of the Sunwapta River, Alberta, Canada*. Earth Surf. Process. Landforms 13, 599–618. https://doi.org/https://doi.org/10.1002/esp.3290130705

Desjardins, E., van de Wiel, M., & Rousseau, Y. (2020). Predicting, explaining and exploring with computer simulations in fluvial geomorphology. *Earth-Science Reviews*, *209*, 102654. https://doi.org/10.1016/J.EARSCIREV.2018.06.015Duvall, A.R., Harbert, S.A., Upton, P., Tucker, G.E., Flowers, R.M., Collett, C., 2020. *River patterns reveal two stages of landscape evolution at an oblique convergent margin, Marlborough Fault System, New Zealand*. Earth Surf. Dyn. 8, 177–194. https://doi.org/10.5194/esurf-8-177-2020

Feeney, C. J., Chiverrell, R. C., Smith, H. G., Hooke, J. M., & Cooper, J. R. (2020). Modelling the decadal dynamics of reach-scale river channel evolution and floodplain turnover in CAESAR-Lisflood. *Earth Surface Processes and Landforms*, *45*(5), 1273–1291. https://doi.org/10.1002/ESP.4804

Geographx, 2012. *NZ 8m Digital Elevation Model*.

Gran, K.B., Czuba, J.A., 2017. *Sediment pulse evolution and the role of network structure*. Geomorphology 277, 17–30. https://doi.org/https://doi.org/10.1016/j.geomorph.2015.12.015

Hancock, G.R., J.B.C., L., Coulthard, T.J., 2015. *Catchment reconstruction — erosional stability at millennial time scales using landscape evolution models*. Geomorphology 231, 15–27. https://doi.org/10.1016/J.GEOMORPH.2014.10.034

Hancock, G.R., Coulthard, T.J., Martinez, C. and Kalma, J.D., 2011. An evaluation of landscape evolution models to simulate decadal and centennial scale soil erosion in grassland catchments. *Journal of Hydrology*, *398*(3-4), pp.171-183.

Hancock, G.R., Verdon-Kidd, D., Lowry, J.B.C., 2017. *Soil erosion predictions from a landscape evolution model – An assessment of a post-mining landform using spatial climate change analogues*. Sci. Total Environ. 601–602, 109–121. https://doi.org/10.1016/J.SCITOTENV.2017.04.038

Heasley, E.L., Clifford, N.J., Millington, J.D.A., 2019. *Integrating network topology metrics into studies of catchment-level effects on river characteristics*. Hydrol. Earth Syst. Sci. 23, 2305–2319. https://doi.org/10.5194/hess-23-2305-2019

Heckmann, T., Cavalli, M., Cerdan, O., Foerster, S., Javaux, M., Lode, E., Smetanová, A., Vericat, D., & Brardinoni, F. (2018). Indices of sediment connectivity: opportunities, challenges and limitations. Earth-Science Reviews, 187, 77-108.

Henshaw, A.J., Sekarsari, P.W., Zolezzi, G., Gurnell, A.M., 2020. *Google Earth as a data source for investigating river forms and processes: Discriminating river types using form-based process indicators*. Earth Surf. Process. Landforms 45, 331–344. https://doi.org/10.1002/ESP.4732

Hey, R.D., Thorne, C.R., 1986. *Stable Channels with Mobile Gravel Beds*. J. Hydraul. Eng. 112, 671–689. https://doi.org/10.1061/(ASCE)0733-9429(1986)112:8(671)

Horton, R.E., 1945. *Erosional Development of Streams and Their Drainage Basins; Hydrophysical approach to quantitative morphology*. Bull. Geol. Soc. Am. 56, 275–370. https://doi.org/https://doi.org/10.1130/0016-7606(1945)56[275:EDOSAT]2.0.CO;2

Hovius, N., Stark, C.P., Tutton, M.A., Abbott, L.D., 1998. *Landslide-driven drainage network evolution in a pre-steady state mountain belt: Finisterre Mountains, Papua New Guinea*. Geology 26, 1071–1074. https://doi.org/https://doi.org/10.1130/0091-7613(1998)026<1071:LDDNEI>2.3.CO;2

James, L.A., 2010. *Secular Sediment Waves, Channel Bed Waves, and Legacy Sediment*. Geogr. Compass 4, 56–598. https://doi.org/10.1111/j.1749-8198.2010.00324.x

Jerolmack, D.J., Paola, C., 2010. *Shredding of environmental signals by sediment transport*. Geophys. Res. Lett. 37. https://doi.org/10.1029/2010GL044638

Knighton, A.D., 1989. *River adjustment to changes in sediment load: The effects of tin mining on the Ringarooma River, Tasmania, 1875–1984*. Earth Surf. Process. Landforms 14, 333–359. https://doi.org/10.1002/esp.3290140408

Knighton, A.D., 1980. *Longitudinal changes in size and sorting of stream-bed material in four English rivers*. Geol. Soc. Am. Bull. 91, 55–62. https://doi.org/10.1130/0016-7606(1980)91<55:LCISAS>2.0.CO;2

Lamb, R., Beven, K.J., 1997. *Using interactive recession curve analysis to specify a general catchment storage model*. Hydrol. Earth Syst. Sci. 1, 101–113. https://doi.org/10.5194/hess-1-101-1997

Larsen, L., Thomas, C., Eppinga, M., & Coulthard, T. (2014). Exploratory Modeling: Extracting Causality From Complexity. *Eos, Transactions American Geophysical Union*, *95*(32), 285–286. https://doi.org/10.1002/2014EO320001

Lisle, T.E., Cui, Y., Parker, G., Pizzuto, J.E., Dodd, A.M., 2001. *The dominance of dispersion in the evolution of bed material waves in* *gravel-bed rivers*. Earth Surf. Process. Landforms 26, 1409–1420. https://doi.org/10.1002/esp.300

Liu, B., Coulthard, T.J., 2017. *Modelling the interaction of aeolian and fluvial processes with a combined cellular model of sand dunes and river systems*. Comput. Geosci. 106, 1–9. https://doi.org/10.1016/J.CAGEO.2017.05.003

Meade, R.H., 1985. *Wavelike movement of bedload sediment, East Fork River, Wyoming*. Environ. Geol. Water Sci. 7. https://doi.org/https://doi.org/10.1007/BF02509922

Rice, S.P., 2017. *Tributary connectivity, confluence aggradation and network biodiversity*. Geomorphology 277, 6–16. https://doi.org/10.1016/j.geomorph.2016.03.027

Rice, S. P. (2007). Aggradation at Tributary Confluences as a Control on Biodiversity in River Networks. *AGUFM*, *2007*.

Rice, S.P., 1998. *Which tributaries disrupt downstream fining along gravel-bed rivers?* Geomorphology 22, 39–56. https://doi.org/10.1016/S0169-555X(97)00052-4

Rice, S.P., Church, M., 1998. *Grain Size Along Two Gravel-Bed Rivers: Statistical Variation, Spatial Pattern and Sedimentary Links*. Earth Surf. Process. Landforms 23, 345–363. https://doi.org/https://doi.org/10.1002/(SICI)1096-9837(199804)23:4<345::AID-ESP850>3.0.CO;2-B

Schmitt, R.J.P., Bizzi, S., Castelletti, A., 2016. *Tracking multiple sediment cascades at the river network scale identifies controls and emerging patterns of sediment connectivity*. Water Resour. Res. 52, 3941–3965. https://doi.org/10.1002/2015WR018097

Schumm, S. A. (1977). *The Fluvial System*. Wiley & Sons Ltd.

Shreve, R.L., 1967. *Infinite Topologically Random Channel Networks*. J. Geol. 75, 178–186. https://doi.org/https://doi.org/10.1086/627245

Sklar, L.S., Dietrich, W.E., Foufoula-Georgiou, E., Lashermes, B., Bellugi, D., 2006. *Do gravel bed river size distributions record channel network structure?* Water Resour. Res. 42, W06D18. https://doi.org/10.1029/2006WR005035

Sklar, L.S., Fadde, J., Venditti, J.G., Nelson, P., Aleksandra Wydzga, M., Cui, Y., Dietrich, W.E., 2009. *Translation and dispersion of sediment pulses in flume experiments simulating gravel augmentation below dams*. Water Resour. Res. 45, 1–14. https://doi.org/10.1029/2008WR007346

Strahler, A.N., 1957. *Quantitative Analysis of Watershed Geomorphology*. EOS, Trans. Am. Geophys. Union 38, 913–920. https://doi.org/10.1029/TR038i006p00913

Tangi, M., Schmitt, R., Bizzi, S., Castelletti, A., 2019. *The CASCADE toolbox for analyzing river sediment connectivity and management*. Environ. Model. Softw. 119, 400–406. https://doi.org/10.1016/j.envsoft.2019.07.008

Tokunaga, E., 1978. *Consideration of the composition of drainage networks and their evolution*. Geogr. Reports Tokyo Metrop. Univ. 13, 1–27.

Viaplana-Muzas, M., Babault, J., Dominguez, S., Van Den Driessche, J., Legrand, X., 2015. *Drainage network evolution and patterns of sedimentation in an experimental wedge*. Tectonophysics 664, 109–124. https://doi.org/10.1016/J.TECTO.2015.09.007

Walley, Y., Henshaw, A.J., Brasington, J., 2020. *Topological structures of river networks and their regional‐scale controls: a multivariate classification approach*. Earth Surf. Process. Landforms 45, 2869–2883. https://doi.org/10.1002/esp.4936

Walley, Y., Tunnicliffe, J.F., Brierley, G.J., 2018. *The influence of network structure upon sediment routing in two disturbed catchments, East Cape, New Zealand*. Geomorphology 307, 38–49. https://doi.org/10.1016/J.GEOMORPH.2017.10.029

Xie, J., Wang, M., Liu, K., Coulthard, T.J., 2018. *Modelling sediment movement and channel response to rainfall variability after a major earthquake*. Geomorphology 320, 18–32. https://doi.org/10.1016/J.GEOMORPH.2018.07.022

Zanardo, S., Zaliapin, I., Foufoula-Georgiou, E., 2013. *Are American rivers Tokunaga self-similar? New results on fluvial network topology and its climatic dependence*. J. Geophys. Res. Earth Surf. 118, 166–183. https://doi.org/10.1029/2012JF002392